

4
5
6
**BEHAVIOR OF COLUMNS CONFINED WITH FRP FABRICS
UNDER REPEATED LATERAL LOADS**

7 **Abstract**

8 The axial strength of reinforced concrete columns is enhanced by wrapping them with Fiber Reinforced
9 Polymers, FRP, fabrics. The efficiency of such enhancement is investigated for columns when they are
10 subjected to repeated lateral loads accompanied with their axial loading. The current research presents that
11 investigation for glass and carbon FRP strengthening as well. The reduction of axial loading capacity due to
12 repeated loads is evaluated. The number of applied FRP plies with different types (GFRP or CFRP) are
13 considered as parameters in our study. The study is evaluated experimentally and numerically. The numerical
14 investigation is done using ANSYS software. The experimental testing are done on five half scale reinforced
15 concrete columns. The loads are applied into three stages. Axial load are applied on specimen in stage 1 with a
16 value of 30% of the ultimate column capacity. In stage 2, the lateral loads are applied in repeated manner in the
17 existence of the vertical loads. In the last stage the axial load is continued till the failure of the columns. The
18 final axial capacities after applying the lateral action, mode of failure, crack patterns and lateral displacements
19 are recorded. Analytical comparisons for the analyzed specimens with the experimental findings are done. It is
20 found that the repeated lateral loads decrease the axial capacity of the columns with a ratio of about
21 (38%-50%). The carbon fiber achieved less reduction in the column axial capacity than the glass
22 fiber. The column confinement increases the ductility of the columns under the lateral loads.
23

24 **1 INTRODUCTION**

25 Confinement of columns is a way to enhance the axial capacity of concrete columns. Many of existing
26 structures have a lack in reinforcement details to resist the seismic loads since they were built before
27 the seismic code requirements are set. Therefore; those existing structures should be upgraded to
28 sustain any increase in stresses due to earthquakes or any lateral loads. Numerous studies have
29 been done about retrofitting columns against earthquakes either by traditional techniques (concrete
30 jackets – steel jackets) [1, 2, 3, 4, 5] or by confining with Fiber Reinforced Polymer fabrics (FRP). S.
31 Memon et al [6] 2005, tested eight specimens under axial compression loads and cyclic lateral
32 displacements. The test results showed that ductility, shear and moment capacities was enhanced by
33 retrofitting columns with GFRP wraps, also the cyclic behavior was improved with increase the
34 number of GFRP layers.
35

36 Stathis and Michael [7] 2003, presented an experimental study for retrofitting columns with concrete
37 jacket and fiber wrapping to study the effect of jacketing under cyclic loading on lacking of lap splices.
38 The test results showed that jacketing is a very effective way of enhancing the deformation capacity of
39 columns. Hamid Saadatmanesh et al [8] 1997, tested four columns up to failure under cyclic loading,
40 then columns were repaired with FRP wraps and re-tested under simulated earthquake loading.
41 Results showed that both flexural strength and displacement ductility of repaired columns were higher
42 than those of the original columns.

43 **2 OBJECTIVE**

44 The main objective is to evaluate the reduction of the axial capacity of strengthened columns after
45 they are subjected to repeated lateral loads. Experimental and analytical studies are carried out on
46 columns confined with two types of FRP fabrics. The variable parameters utilized in our study are:

47 the type of confinement material, carbon or glass FRP fabrics, and the number of the applied FRP
48 plies: one or two.

49
50 The behaviour of such strengthening is examined through tracing the cracks' pattern, measuring the
51 lateral displacements and the axial capacity of tested columns. The loads are applied into three stages.
52 Axial load are applied on specimen in stage 1 with a value of 30% of the ultimate column capacity. In stage 2,
53 the lateral loads are applied in repeated manner in the existence of the vertical loads. In the last stage the axial
54 load is continued till the failure of the columns. Then, those columns are numerically examined using a
55 general purpose finite element program, ANSYS. The numerical model is compared with the
56 experimental findings.

58 3 EXPERIMENTAL PROGRAM

59 The experimental program is done on five half scale reinforced concrete columns. The specimens are
60 investigated for the axial loading capacity after applying repeated lateral loads at the top of the
61 columns. The columns are constructed in the RC laboratory, at Faculty of Engineering, at Matriah,
62 Helwan University. The experimental test program was done under lateral cycles of loading and unloading
63 with the existence of axial load. The specimens are detailed as:

- 64 • A control specimen (without wrapping).
- 65 • Two fully confined specimens with glass fiber (single and double wrapping).
- 66 • Two fully confined specimens with carbon fiber (single and double wrapping).

67 3.1 Description of the tested specimens

68 All columns have the same cross-sectional area of 25x25 cm, the same height of 150 cm, the same
69 reinforcement ratio, and the same footing dimensions. The details of the specimen reinforcement is shown in
70 Figure (1). Three standard cubes for each column were tested after 28 days for the material compressive
71 strength. The average compressive strength of the cubes is 30 MPa. The columns are reinforced with
72 vertical bars of 6T12. Closed stirrups of 5R8/m are built as shown (T and R) represent steel material with
73 yield strength of $f_y=360$ and 240 MPa respectively. The columns are fully wrapped with GFRP and CFRP
74 fabrics. The specimens are divided into three categories. One column is built without fiber
75 wrapping. This column is used as a control specimen. Two columns are built and then confined with glass
76 FRP warping by one or two layers. Similar columns are built and then confined with carbon FRP warping
77 by one or two layers. The details of the specimens are shown in Table (1).

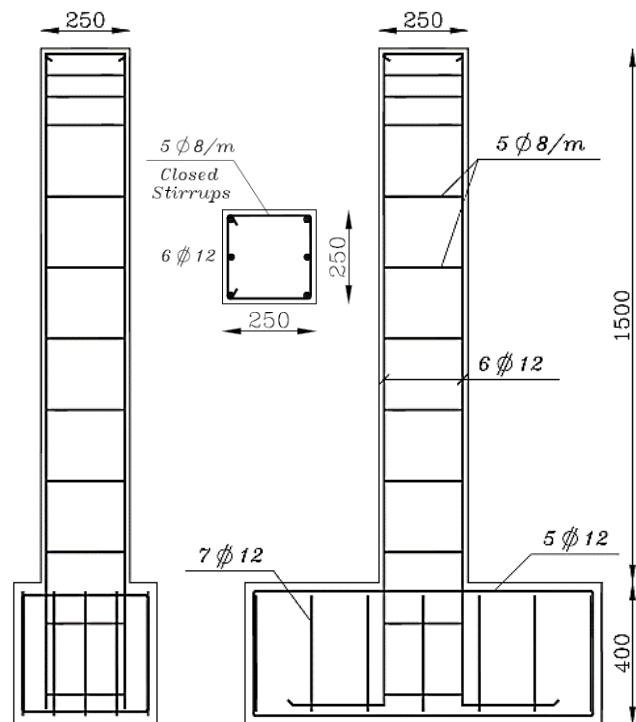


Figure 1: Dimension of the specimens and reinforcement details

88
89
90
91
92
93
94
95

96 Table 1: Details of the column specimens

Column	Cross section (mm)	Height (mm)	Footing (mm)	Columns ' RFT Ratio %	Columns ' RFT	Stirrups	No. and types of FRP Plies
C2	250x250	1500	400x1000x400	1.08 %	6T12	5R8/m (Closed)	----
C2G1				1.08 %	6T12	5R8/m (Closed)	1 Ply GFRP
C2G2				1.08 %	6T12	5R8/m (Closed)	2 Plies GFRP
C2C1				1.08 %	6T12	5R8/m (Closed)	1 Ply CFRP
C2C2				1.08 %	6T12	5R8/m (Closed)	2 Plies CFRP

97 **3.2 Properties of the used materials**

98

99 The used concrete mixture are designed and used for the column specimens at the faculty laboratory. Three
 100 standard cubes for each column were tested after 28 days for the material compressive strength. The average
 101 compressive strength of the cubes is 30 MPa. The columns are fabricated with main steel reinforcement bars
 102 having a yield strength of $f_y=360$ MPa. The yield strength of the stirrups is 240 MPa. The columns are
 103 wrapped with CFRP and GFRP fabrics with physical properties as shown in Table 2. The epoxy is used as an
 104 adhesive material with properties shown in Table 3.
 105

106 Table 2: Physical properties of the FRP material

	CFRP Fabrics Sikawrap-300C	GFRP Fabrics Sikawrap-430G
Product Label	Sikawrap-300C	Sikawrap-430G
Product Description	Unidirectional, woven carbon fiber	Unidirectional, woven glass fiber
Fabric length/roll	≥ 50 m	≥ 50 m
Fabric width	300/600 mm	600 mm
Density	1.82 g/cm ³	2.56 g/cm ³
Fabric design thickness	0.167 mm	0.168 mm
Tensile strength of fiber	4000 N/mm ²	2500 N/mm ²
Tensile E-modulus of fiber	230000 N/mm ²	72000 N/mm ²
Strain at break of fiber	1.7 %	2.7 %

107

108

109 Table 3: Properties of the adhesive material

	Epoxy Sikadur-330
Product Label	Sikadur-330
Product Description	Sikadur-330 is a two-part, thixotropic epoxy based impregnating resin / adhesive
Appearance / Colors	Resin part A: Paste, Hardener part B: Paste Part A: white, Part B: grey Part A + Part B mixed: light grey
Mixing Ratio	4 (Part A): 1 (Part B)
Tensile strength	30 N/mm ²
Bond strength	Concrete fracture (> 4 N/mm ²)
Tensile E-modulus	3800 N/mm ²
Strain at break of fiber	0.9 %

110 **4 Test Setup**

111 All experiments have been carried out in the Faculty of
 112 Engineering – Helwan University – Mattaria Branch.
 113 Our specimens were installed on a heavy steel frame.
 114 The footing was supported on the frame as a fixed
 115 support with four steel rods, and the top of the column
 116 was set to be free. A steel cap was placed at the top of
 117 the column in order to prevent crushing beyond the
 118 load cell. Two jacks were used: vertical jack for
 119 applying vertical axial load, and horizontal jack for
 120 applying horizontal load. Each jack applied its load on
 121 a load cell which can read the load value. Figure (2)
 122 shows the test set-up.



Figure 2: Test setup

123 4.1 Measurements

124 *Measuring the horizontal displacement:*

125 Three Linear Voltage Displacement Transducers,
 126 LVDTs, are placed along the column height at Levels
 127 (0.25, 0.5, and 0.75) of the column height. Also,
 128 additional LVDT is placed at the level of acting of the
 129 horizontal load cell as shown in figure (2).

130 *Measuring the loads:*

132 The vertical and the horizontal loads are measured
 133 using load cells.

134 *Measuring the strains in the reinforcement bars*

135 Electrical strain gauges are attached to the vertical
 136 reinforcement bars to measure their strains. The strain
 137 gauges type has gauge lengths of 6mm, the gauge
 138 resistance is 120.3 ± 0.50 ohm, and the gauge factor is
 139 2.12 ± 1.0 %. For each column four strain gauges were
 140 installed. Two of them were placed in the column's
 141 reinforcement just above the footing by 5 cm in the
 142 vertical direction whereas the other two gauges were
 143 placed with 20 cm in above on the same bar. The
 144 strain gauges are connected to a strain meter device
 145 with accuracy of 1×10^{-6} .



Figure 3: Strain Gauge locations

146 4.2 Testing Procedure

147 The testing is done in according to the following steps:

148 1. The vertical load is applied gradually up to 30% of
 149 the ultimate axial strength of the column cross
 150 section. Those values are calculated for each
 151 specimen considering the confinement effect.
 152 That load is kept constant during step 2 of the test.

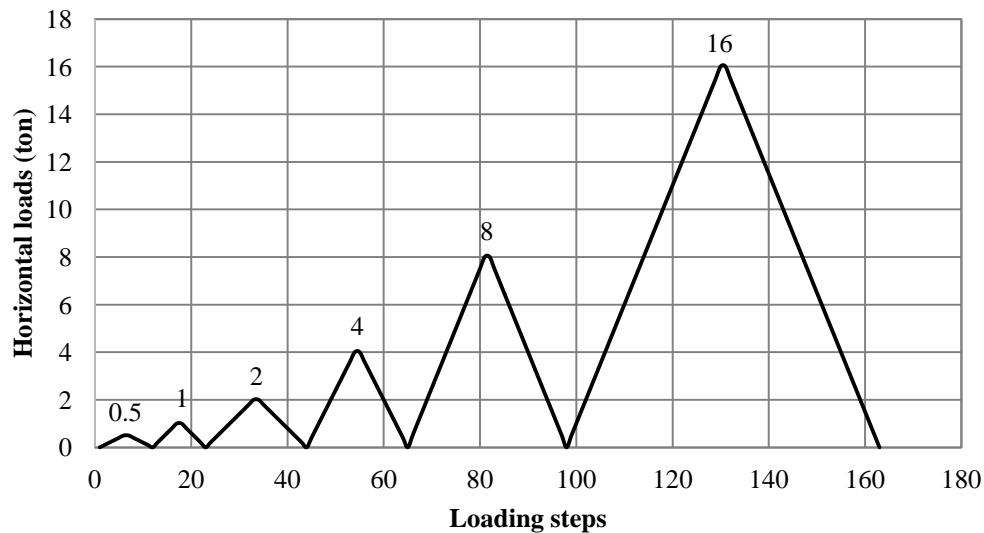
153 2. The horizontal load is applied after step 1 and increased gradually in cyclic mater. In each cycle
 154 the horizontal load reaches a certain value and then it is released to return to the zero value.
 155 The maximum values for the cycles are set to (0.5, 1, 2, 4, 8 and 16) tons. Figure 5 shows the
 156 planed repeating loading history. The horizontal loads is applied till the loading degradation
 157 (failure condition).



Figure 4: Calibration of the strain gauges

158 3. In this step the horizontal jack is released from the specimens and the axial load is increased
159 gradually up to failure to investigate the maximum axial loading capacity after the failure due to
160 the repeated lateral loads.

161 The results are recorded during the test and several items are recorded: (1) lateral and axial loads at
162 the failure stages, (2) lateral load–displacement curve, (3) failure modes, (4) crack patterns, and (5)
163 deformed shape.
164



165
166

Figure 5: The horizontal loading history plan

167 5 EXPERIMENTAL RESULTS

168 The results of each step of testing are recorded. The cracking pattern for each specimen is
169 documented for step 2,3 of loading. In addition, the relation of the load-horizontal displacement are
170 constructed for each specimens.

171 5.1 Cracking pattern

172 The crack pattern is recorded at the end of step 2 where the column has lost its strength due to the
173 lateral loads. Also, the cracks are recorded at the end of step 3 where the axial load is applied till the
174 axial failure of the tested column. Figures 6 to 16 shows the cracks distributions.

175
176
177
178
179
180
181
182
183
184
185
186
187
188
189
190
191
192
193



Figure 6: The cracks of C2 column under the lateral loads



Figure 7: The cracks of column C2 at failure under the ultimate axial load



Figure 8: The cracks of column C2G2 at failure under the ultimate axial load



Figure 10: The cracks of column C2G1 at failure under the ultimate axial load

211



Figure 11: The cracks of C2G2 column at failure under the lateral load. Separation of the fiber is

226
227



Figure 9: The cracks of C2G1 column at failure under the lateral load. Separation of the fiber is noticed.



Figure 12: The cracks of column C2C1 at failure under the ultimate axial load

248
249

Figure 13: The cracks of C2C1 column at failure under the lateral load. Separation of the fiber is noticed

250
251
252
253
254
255
256
257
258
259
260
261
262
263
264
265
266
267
268
269
270
271
272
273
274
275
276
277
278
279
280

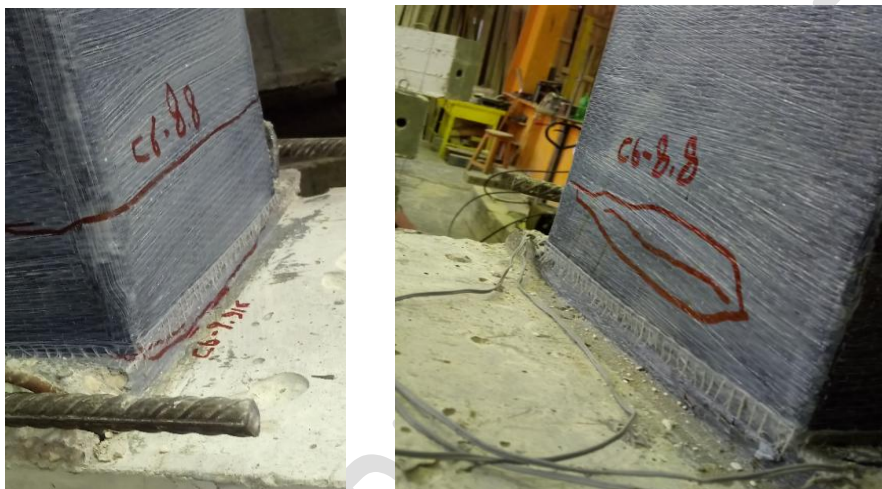


Figure 14: The cracks of C2C2 column at failure under the lateral load. Separation of the fiber is noticed at the marked area.

281
282
283
284
285
286
287
288

5.2 Load-horizontal displacement relationship (step 2 loading)

The horizontal load versus the displacement at the level of the acting load is graphed for each specimens. It is clear that the horizontal response of each specimen is influenced by the amount of the axial loading applied on the specimens.

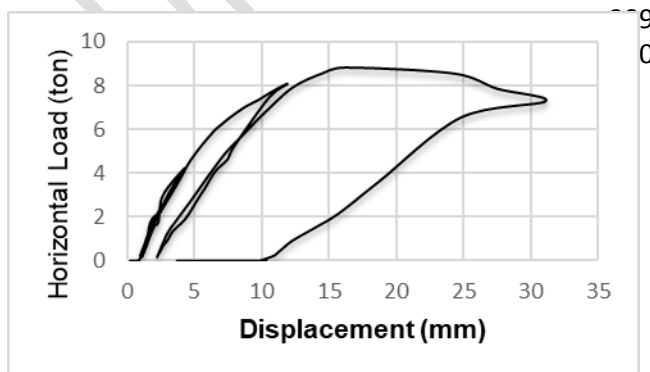


Figure 15: The load displacement relation for C2C1

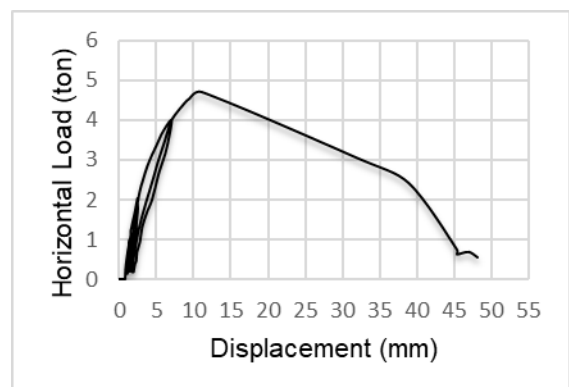


Figure 16: The load displacement relation for C2G2

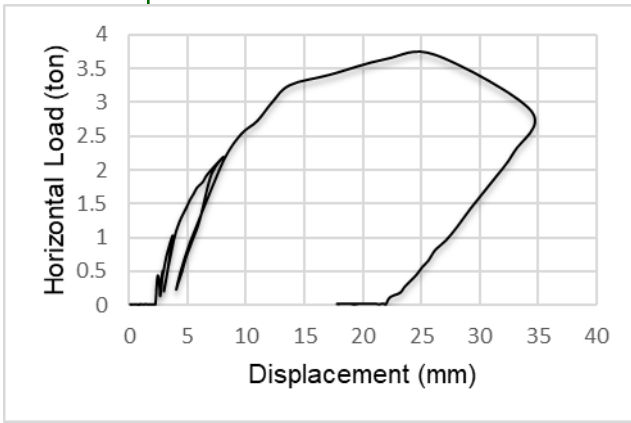


Figure 18: The load displacement relation for C2G1

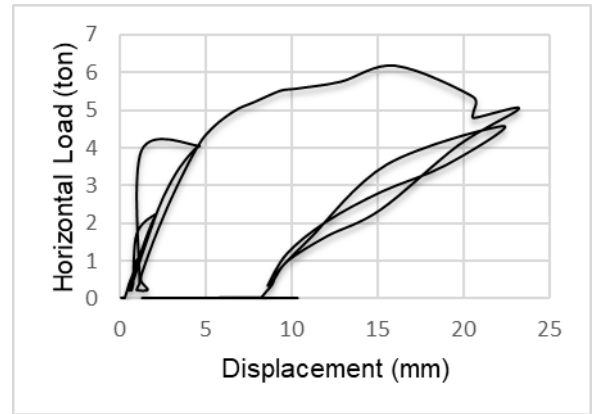


Figure 17: The load displacement relation for C2

291

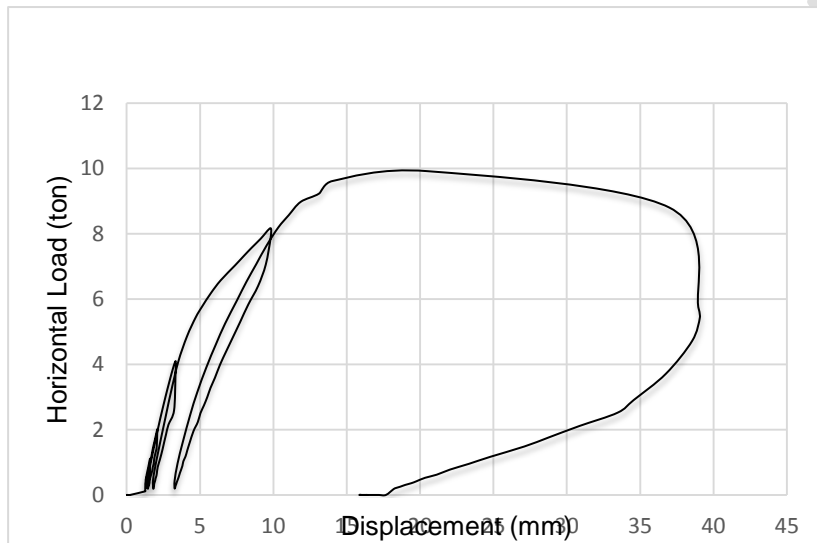


Figure 19: The load displacement relation for C2C2

292
293
294
295
296
297
298
299
300
301
302
303
304
305
306
307
308
309
310
311
312
313
314
315

In addition, the maximum horizontal load is measured at each cycle for the specimens during testing. Also, the axial load is maintained constant during step 2 of testing for each test. That axial load represent almost 30% of the calculated ultimate load for each column including the confinement effect. Those values are shown in Table 4.

Table 4: The maximum recorded horizontal load for each cycles

Specimen	Cycle 1	Cycle 2	Cycle 3	Cycle 4	Cycle 5	Cycle 6	Max Hz load	Axial app. Load (step 2)
C2	0.494	1.064	2.223	4.047	6.175	Test end	6.175	30.7
C2G1	0.503	1.024	2.19	3.7	Test end	Test end	3.700	38.5
C2G2	0.592	0.994	2.036	4.007	Test end	Test end	4.007	39.9
C2C1	0.526	1.065	2.089	4.232	8.057	8.803	8.803	43.4
C2C2	0.538	1.112	2.012	4.09	8.169	9.916	9.916	52.4

316
317
318

From the above relations one can notice that the confinement of the samples has improved the ductility criteria since the lateral displacement is increased. That is shown for the specimens with 2

plies have more displacements than specimens with one ply by 18% and 29% for glass and carbon fiber consequently.

5.3 Column axial Capacity (step 3 loading)

The horizontal repeated loads were applied on specimens till load degradation. In step 3, the horizontal loads are removed and then the axial load is increased till failure of the specimens. The maximum values of that axial load is compared with the calculated nominal value of the axial strength of such section without any lateral loads' history. That is shown in the Figure 20. That figure shows that the axial capacity has lost about 50% of their nominal axial strength. You may notice that specimens confined with CFRP layers have the least reduction.

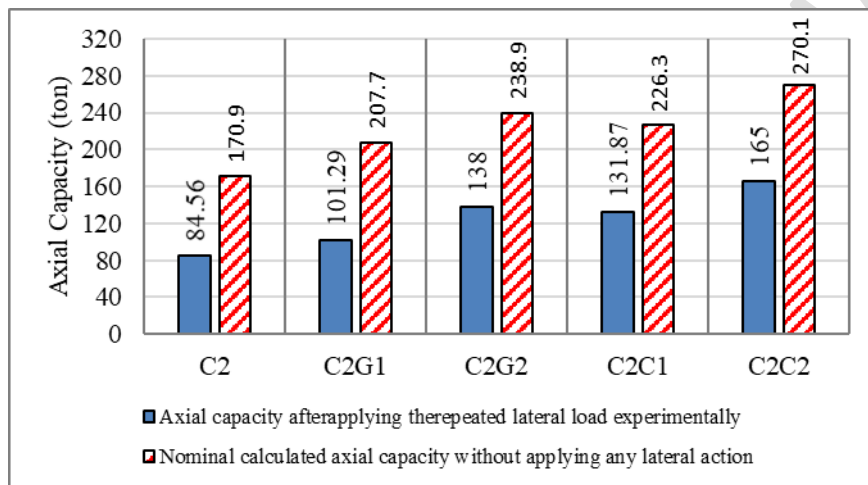


Figure 20: maximum axial loads after step 3 of loading

6 NUMERICAL INVESTIGATION

The general purpose finite element program is utilized in our study. The experimented specimens are modeled and tested in the same procedures as they are tested. The concrete material is modelled using element SOLID 65. The element is defined by eight nodes having three degrees of freedom at each node: translations in the nodal x, y, and z directions. The solid is capable of cracking in tension and crushing in compression. The FRP material is modeled using SOLID185, see Figures (21 to 24). In addition, the reinforcement bars are modeled using element link180. The element is defined by eight nodes having three degrees of freedom at each node: translations in the nodal x, y, and z directions. The layered composite specifications including layer thickness, material, orientation, and number of integration points through the thickness of the layer are specified via shell element. CONTA173 is used to represent contact and sliding between 3-D solid element and a deformable surface. This element has three degrees of freedom at each node: translations in the nodal x, y, and z directions. The following figures illustrates the meshing and the reinforcement details.

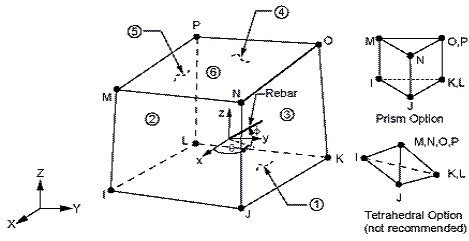
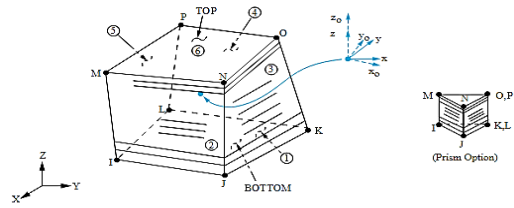


Figure 21: Solid 65 element



x_0 = Element x-axis if ESYS is not supplied.
 x = Element x-axis if ESYS is supplied.

Figure 22: Solid 185 element

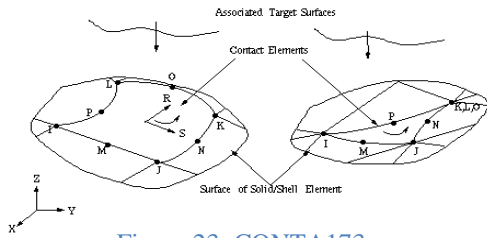


Figure 23: CONTA173

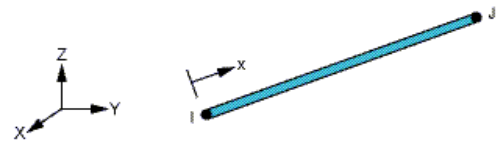


Figure 22: Link 180 element

- 359
- 360
- 361
- 362
- 363
- 364
- 365
- 366
- 367
- 368
- 369
- 370
- 371
- 372
- 373
- 374
- 375
- 376
- 377
- 378
- 379
- 380
- 381
- 382
- 383
- 384
- 385
- 386
- 387
- 388
- 389

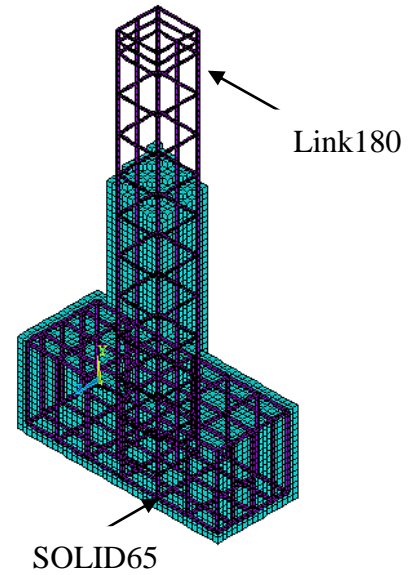
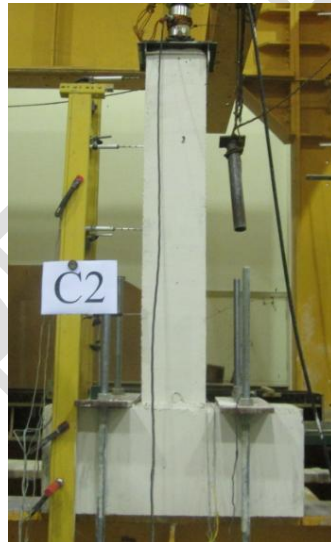
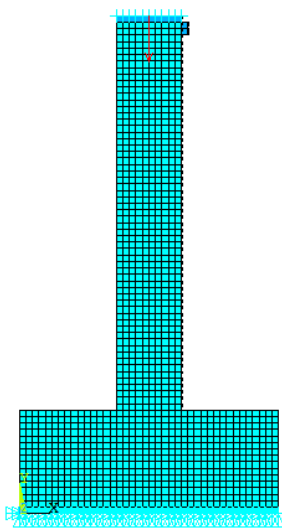


Figure 23: Finite Element Model for Unconfined Column

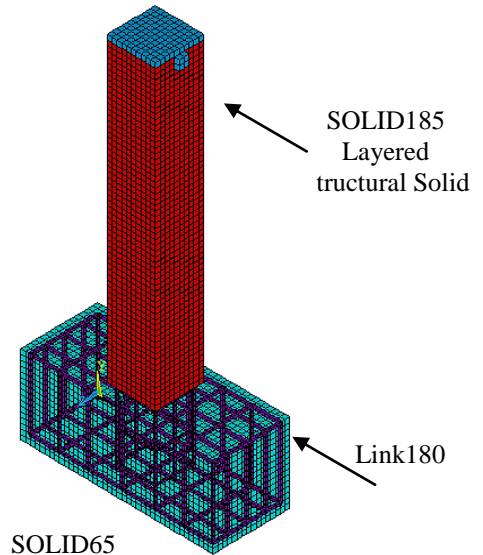
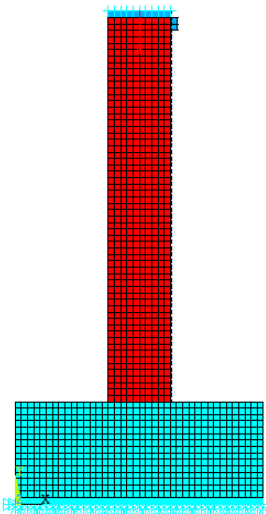


Figure 24: Finite Element Model for confined Column

390

391 7 RESULTS OF THE NUMERICAL STUDY

392 7.1 Lateral strength of the models (step 2 of loading)

393

394 The vertical loads in addition to the horizontal load history is applied to the numerical models as done for the
395 experimented specimens. The application continue until degradation of the horizontal strength. Then after the
396 axial load is applied till failure of the models. Table 5 shows the maximum horizontal forces for the
397 experimented specimens and the numerical models. It is noted that the experimental results with the numerical
398 models are in good agreement.

399

400

401

Table 5: Lateral Capacities of Columns from ANSYS (P_{hANS}) and Experiment (P_{hEXP})

Column	Pv, Axial app. Load (step 2) (ton)	Loaded horz. till cycle no	P_{hANS} (ton)	P_{hEXP} (ton)	P_{hANS}/P_{hEXP}
C2	30.7	5	6.065	6.175	98%
C2G1	38.5	4	3.990	3.700	108%
C2G2	39.9	4	4.000	4.007	100%
C2C1	43.4	6	7.800	8.803	89%
C2C2	52.4	6	7.870	9.916	79%

402 7.2 Axial strength of the models (step 3 of loading)

403 The maximum axial load is measured at failure (at the end of step 3 of loading) and presented for all specimens
404 in the Table 6. It is noted that the experimental results with the numerical models are in good agreement.
405 Figure 27 shows the axial strength of specimens with lateral repeated load history. Those values are compared
406 with the values calculated from the ANSYS model. Good agreement is found between the numerical and the
407 experimental findings. The variation was in the range of (2%-10%) whereas the ANSYS values are always
408 higher. Also, the maximum nominal strength for the specimens is calculated and compared with the ANSYS
409 findings. Those values are close.

410

411

Table 6: Axial Capacities of Columns from ANSYS (P_{ANS}) and Experiment (P_{EXP})

Column	P_{vANS} (ton)	P_{vEXP} (ton)	P_{vANS}/P_{vEXP}
C2	90.13	84.56	1.07
C2G1	110.1	101.29	1.09
C2G2	152	138	1.101
C2C1	135.1	131.87	1.02
C2C2	170	165	1.03

412

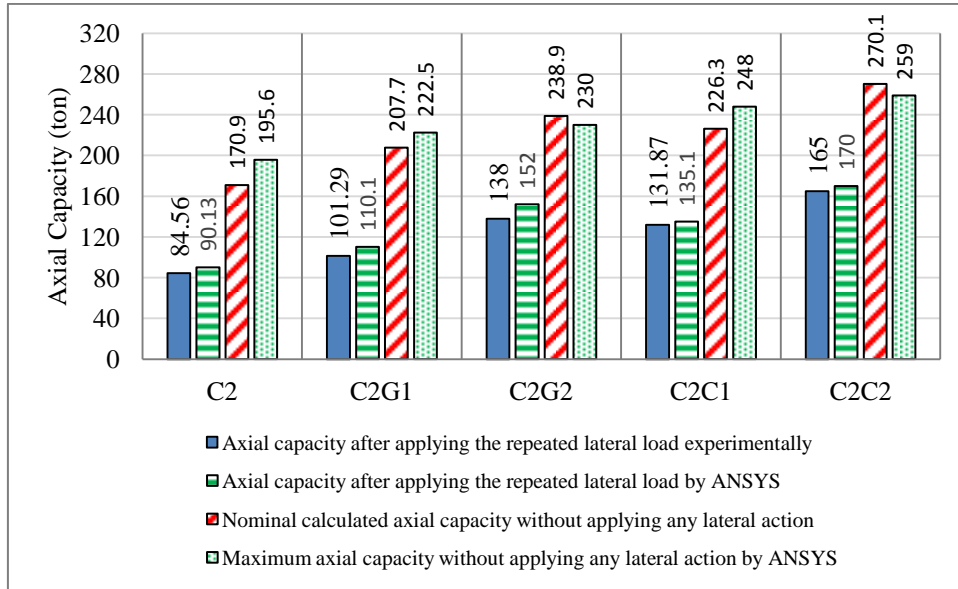


Figure 25: Axial strength values for specimens with and without repeated horizontal loading history

7.3 Cracking Patterns

• Unconfined Column

Figure 28 illustrate the crack patterns occurred in concrete for the unconfined columns due to both lateral and axial loads. There is a match for the crack pattern found in the numerical models with the experimental outcomes all over the loading stages.

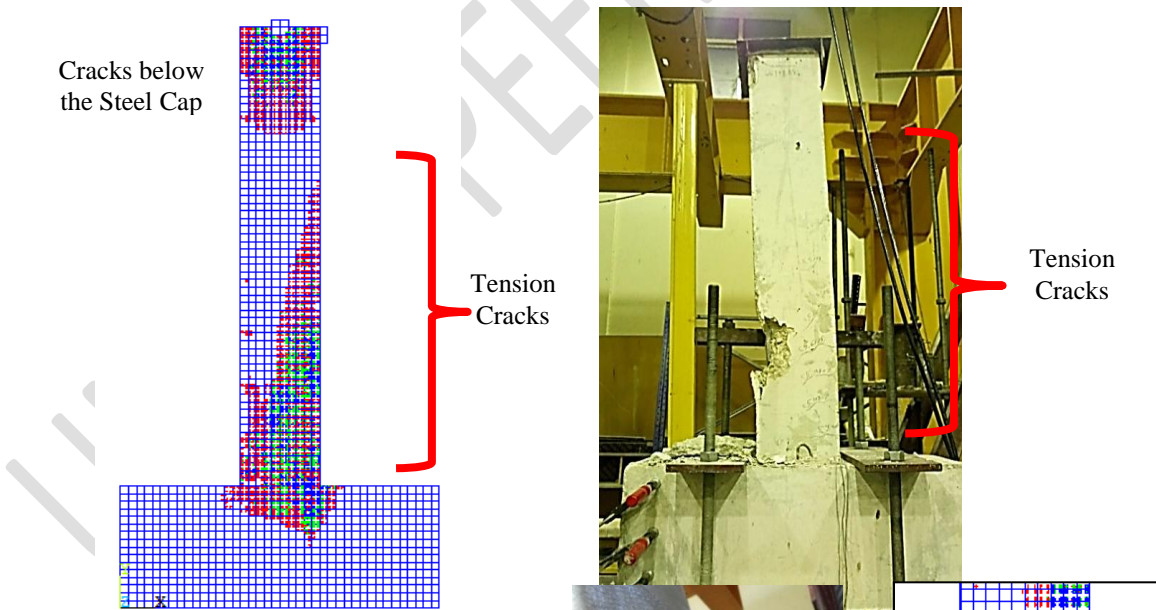


Figure 26: Crack Pattern for Unconfined Column

• Confined Columns

It should be noted that the crack patterns obtained from ANSYS for the confined columns is able to simulate the cracks occurred

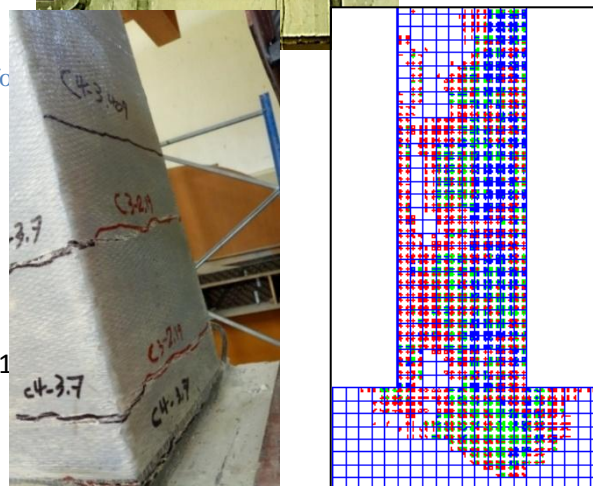


Figure 27: Crack Pattern for Confined Columns

445 in the concrete under the FRP laminates. That is not appear on the photos taken from the
 446 experimental tests because of confinement obstruction. Therefore, the crack patterns obtained from
 447 ANSYS for the confined columns covers larger area than the experimental specimens as shown in
 448 Figure 29.

449
 450
 451

452 The separation of fiber from concrete surface which is occurred in the experimental tests at the lower
 453 third of column in the compression zone. That is notice also in ANSYS models. That is due to
 454 simulating the epoxy material by contact element model as shown in Figure (30).

455
 456
 457
 458
 459
 460
 461
 462

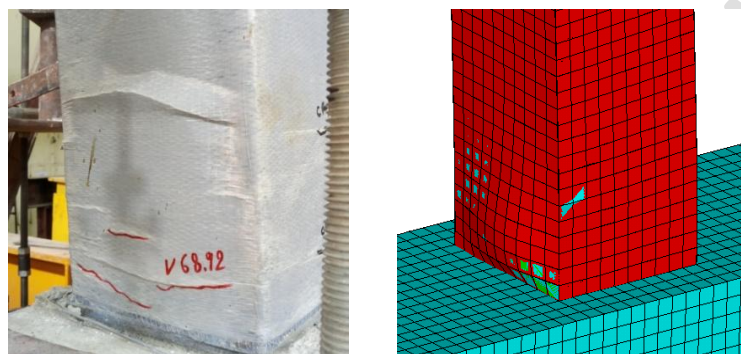


Figure 28: Separation of FRP at the Bottom of Confined Columns

463
 464

7.4 Lateral Load – Displacement Curves

465

466 Comparison of the lateral-load-displacement curves for all specimens from the tests and ANSYS
 467 models are presented in the following figures.

468
 469

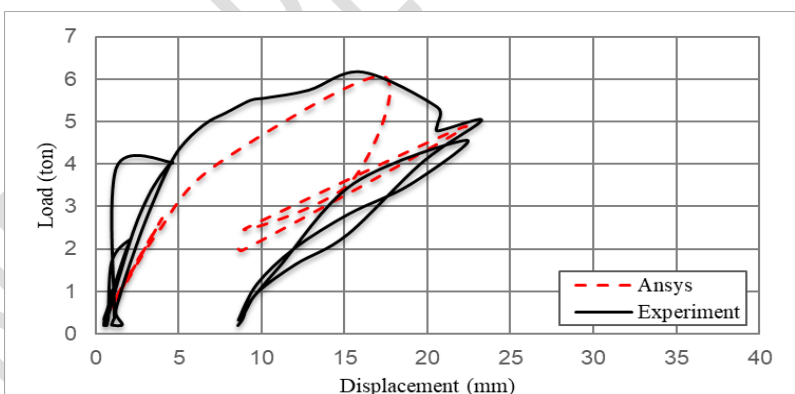


Figure 29: Comparison for P_h – Displacement Curve for C2C1

470
 471
 472
 473
 474
 475
 476

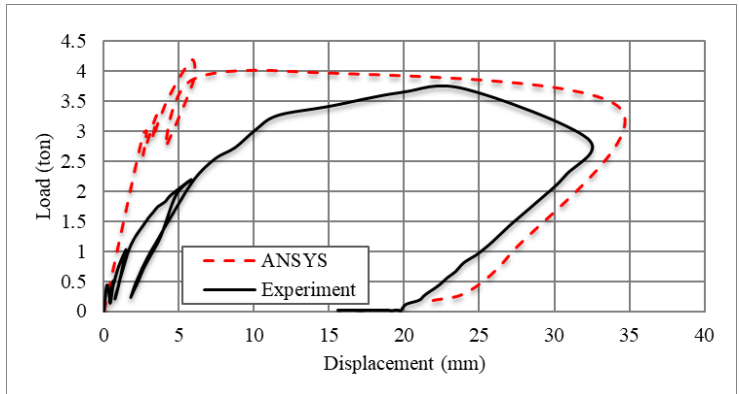


Figure 30: Comparison for P_h – Displacement Curve for C2C1

477
 478
 479
 480
 481
 482
 483

484
485
486
487
488
489
490
491
492
493
494
495
496
497
498
499
500
501
502
503
504
505
506
507
508
509
510
511
512
513
514
515

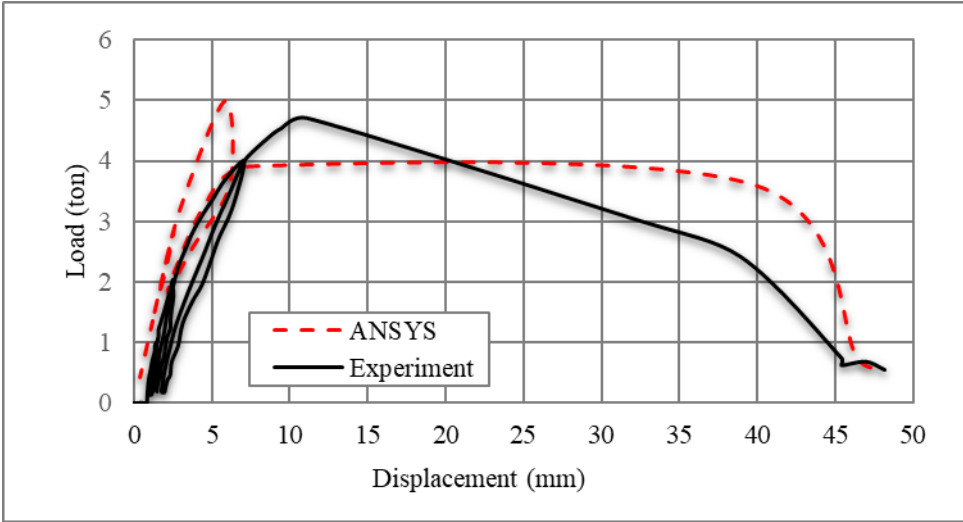


Figure 31: Comparison for P_h – Displacement Curve for C2G2

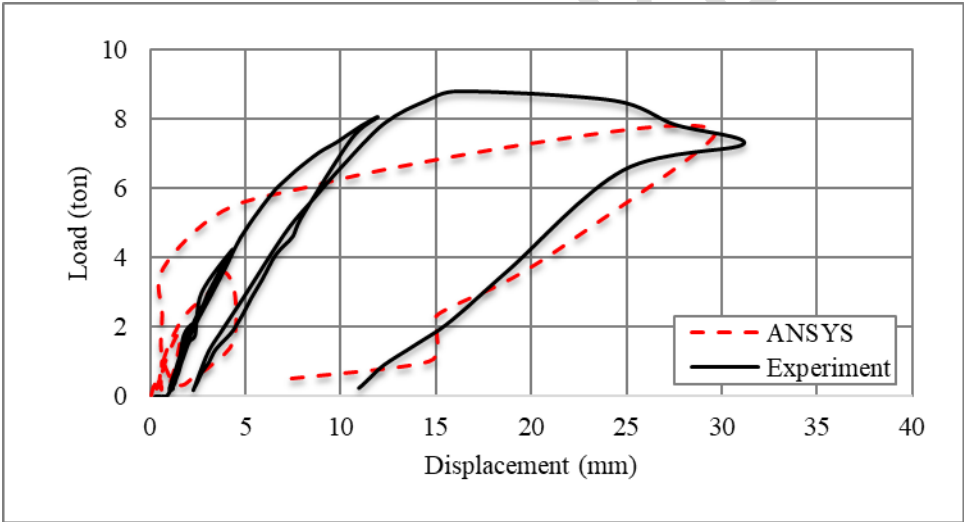


Figure 32: Comparison for P_h – Displacement Curve for C2C1

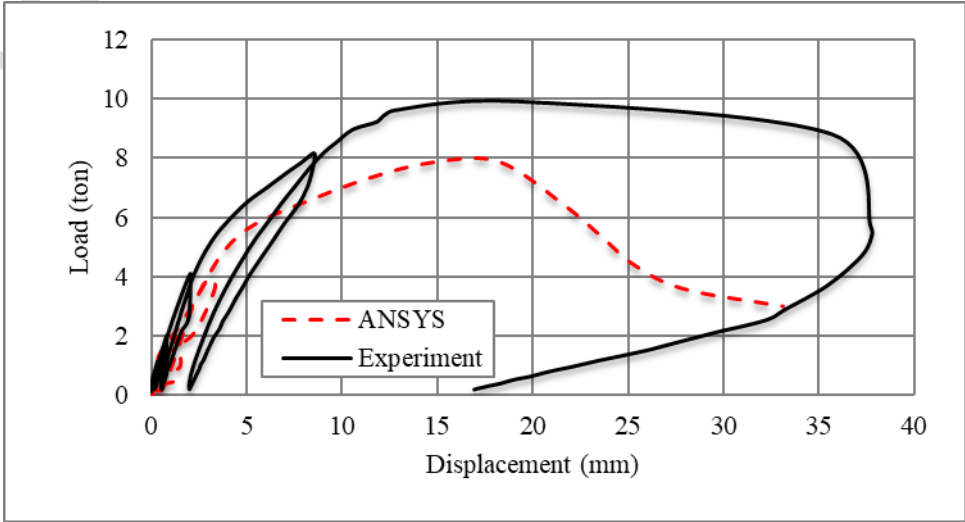


Figure 33: Comparison for P_h – Displacement Curve for C2C2

516

517 From the above figures one can notice that the experimental and the numerical findings are in good agreements.
518 Then the numerical model is valid and give a reasonable results and can be used for further studies with anther
519 parameters.

520 8 CONCLUSION

- 521 1. It is found that the repeated lateral loads decrease the axial capacity of the columns with a ratio of
522 about (38%-50%).
- 523 2. The carbon fiber achieved less reduction in the column axial capacity than the glass fiber.
- 524 3. In general, the column confinement increases the ductility of the columns under the lateral loads.
- 525 4. The increase of the number of plies slightly decreases the reduction in axial capacity due to
526 applying repeated lateral load.
- 527 5. Good agreements are achieved between the experimental and analytical models. Simulating the
528 epoxy material with contact element on the numerical models leads to a realistic performance for
529 the numerical model compared with the real experimented columns.

530 REFERENCES

- 531 1. Shuenn-Yih Chang et al, (2014), "Seismic Retrofitting of RC Columns with RC Jackets and Wing
532 Walls with Different Structural Details", Earthquake Engineering and Engineering Vibration,
533 Vol.13, No.2.
- 534 2. Hamidreza Nasersaeed et al, (2011), "Evaluation of Behavior and Seismic Retrofitting of RC
535 Structures by Concrete Jacket", Asian Journal of Applied Sciences.
- 536 3. Yeou-Fong Li and Jenn-Shin Hwang, (2005), "A Study of Reinforced Concrete Bridge Columns
537 Retrofitted by Steel Jackets", Journal of the Chinese Institute of Engineers, Vol. 28, No. 2.
- 538 4. J H Wang et al, (2005), "Seismic Retrofit of Existing R/C Rectangular Columns with Circular Steel
539 Jackets", 30th Conference on Our World in Concrete & Structures, Singapore.
- 540 5. Guo Z.X. et al, (2008), "Experimental Study on A New Retrofitted Scheme for Seismically
541 Deficient RC Columns", The 14th World Conference on Earthquake Engineering, Beijing, China.
- 542 6. Muhammad S. Memon and Shamim A. Sheikh, (2005), "Seismic Resistance of Square Concrete
543 Columns Retrofitted with Glass Fiber-Reinforced Polymer", ACI Structural Journal.
- 544 7. Stathis N. Bousias and Michael N. Fardis, (2003), "Experimental Research on Vulnerability and
545 Retrofitted of Old-Type RC Columns Under Cyclic Loading", Springer.
- 546 8. Hamid Saadatmanesh et al, (1997), "Repair of Earthquake-Damaged RC Columns with FRP
547 Wraps", ACI Structural Journal.
- 548 9. Mesay A. Endeshaw et al, (2008), "Retrofit of Rectangular Bridge Columns Using CFRP
549 Wrapping" Washington State Transportation Center (TRAC) - Washington State University -
550 Department of Civil & Environmental Engineering.
- 551 10. Z. Yan, C.P. Pantelides, and L.D. Reaveley, (2008), " Seismic Retrofit of Bridge Columns Using
552 Fiber Reinforced Polymer Composite Shells And Shape Modification", The 14th World
553 Conference on Earthquake Engineering.
- 554 11. Brian John et al, (2010), "Seismic Retrofit of Cruciform-Shaped Columns in The Aurora Avenue
555 Bridge Using FRP Wrapping", Washington State University – Department of Civil & Environmental
556 Engineering.
- 557 12. Gnanasekaran and Amlan, (2009), "Seismic Retrofit of Columns in Buildings for Flexure Using
558 Concrete Jacket", ISET Journal of Earthquake Technology, Paper No. 505, Vol. 46, No. 2.